Biointerphases
a SpringerOpen Journal

ORIGINAL ARTICLE Open Access

X-ray and neutron investigation of self-assembled lipid layers on a titanium surface

Maksym Golub[1*], Dieter Lott[1], Erik B Watkins[2], Vasyl Garamus[1], Berengere Luthringer[1], Michael Stoermer[1], Andreas Schreyer[1] and Regine Willumeit[1]

Abstract

Titanium is the most widely preferred metal material for bone reconstruction in orthopedics and dentistry. To improve its biological performance, various coatings can be applied. In this investigation, a biomimetic coating on a model implant surface was studied in X-ray and neutron reflectivity experiments to probe the quality of this coating, which is only few nanometers thick. Titanium was deposited on polished silicon surfaces using a magnetron sputtering technique. To improve the lipid coating's stability, a stronger van der Waals interaction was first created between the implant surface and the biomimetic coating by adding a phosphonic acid (n-octadecylphosphonic acid – OPA) monolayer onto the surfaces. Then, three monolayers of POPE (phospholipid 1-palmitoyl-2-oleoyl-sn-glycero-3-phospho-ethanolamine) were transferred using the Langmuir-Blodgett (LB) and Langmuir-Schaefer (LS) techniques. The analysis of X-ray and neutron specular reflectivity data shows that OPA molecules cover the model implant surface completely and that approximately 50% coverage of POPE can be achieved by LB and LS transfer.

Keywords: Self-assembled monolayer of N-octadecylphosphonic acid; POPE coating; Titanium implants; X-ray and neutron reflectivity

Background

The demands on medical implants as safe and long-term solutions for problems with the musculoskeletal system are rapidly growing due to increased life expectancy, changing lifestyles and improved implant technology [1]. At present, problems related to orthopedic, oral and maxillofacial disorders annually affect millions of patients. The diseases and problems caused by damaged bone tissue represent an worldwide annual cost that now exceeds 40 billion euro [2]. Furthermore, the rapid increase of the number of elderly people due to longer life expectancies and different types of degenerative-dystrophic changes such as osteoarthritis and rheumatoid arthritis [3] require that implants endure longer and perform even when patients have compromised health conditions [4]. Recent scientific discoveries have provided novel insights into the biological mechanisms that are responsible for bone healing [5]. These achievements currently facilitate the development of implants that interact optimally with bone tissue due to a so-called "smart implant surface". As a consequence, implants have become increasingly important in regaining health and improving quality of life.

Any materials that are implanted in bone tissue are required to be non-toxic, non-immunogenic, non-thrombogenic, and non-carcinogenic [6]. In this respect, titanium and its alloys have become preferred materials. The formation of a thin but very stable oxide layer on the surface is responsible for the inertness of these types of implants [7].

Several attempts have been made to develop implant surface modifications that may prolong the lifespan of an implant and ensure faster and more stable implant incorporation, which allows patients to have a shorter recovery time. To obtain biologically active materials that provide biological cues for tissue regeneration, various coatings can be applied [8]. One possible approach is a biomimetic coating based on phospholipids that can induce calcification or better cell differentiation [9-12]. Therefore, biomembranes could serve as a model for the molecular engineering of biocompatible and bioactive surfaces for implantable biomaterials [13].

* Correspondence: Maksym.Golub@hzg.de
[1]Institute of Materials Research, Helmholtz-Zentrum Geesthacht Zentrum für Material und Küstenforschung (HZG), Geesthacht, Germany
Full list of author information is available at the end of the article

Critical issues for these types of surface modifications are the stability of the coating during implantation and its subsequent performance. Phospholipid coatings may not be stable enough in a liquid environment due to their tendency to form micelles, vesicles or other aggregates in water. One possible way to improve the adhesion between the metal surface and the lipids is to create a strong van der Waals interaction between the implant surface and the phospholipid coating. Here, an interface was created by first applying a self-assembled monolayer (SAM) of OPA (n-octadecylphosphonic acid - $C_{18}H_{38}O_3P$) coating prior to Langmuir-Blodgett lipid deposition. The SAM of OPA forms a highly stable phosphate-metal cation under specific conditions (e.g., temperature) as the affinity of the phosphate in the OPA molecule to Ti (IV) is very high. These bonds directly link the phosphate head group to the metal cation through either one oxygen atom (monodentate) or two oxygen atoms (bidentate) [14]. In a subsequent step, phospholipids were added, and the hydrophobic surface formed by the OPA alkyl chains should offer a more stable configuration due to the stronger van der Waals interactions with an adjacent phospholipid monolayer than a native titanium surface [15]. In a subsequent step, the phospholipid POPE is added. Thus, an asymmetric bilayer is formed that is linked to the surface, at the same time it is expected that such an asymmetric bilayer still exhibits the liquid crystalline properties of membranes. This layer serves as the first layer of the biomimetic coating. However, it was deduced from cell culture experiments that even more lipid bilayers, though only weakly bound by hydrophobic-hydrophilic interactions, seem to be present. To elucidate whether this assumption is true and how these layers form, we undertook this study.

In this work, the POPE phospholipid 1-palmitoyl-2-oleoyl-sn-glycero-3-phospho-ethanolamine is used due to its unique biophysical properties such as polymorphism, i.e., the capability to form inverse hexagonal structures that is a prerequisite for cell division [16]. POPE contains the zwiterionic head group phosphatidylethanolamine (PE), which is found in all living cells and composes up to 30% of membrane phospholipids. In human physiology, it is particularly found in nervous tissue such as the white matter of the brain, nerves, neural tissue, and the spinal cord [17]. Additionally, PE is thought to be important in the heart. When blood flow to the heart is restricted, the asymmetrical distribution of PE between membrane leaflets is disrupted, and the membrane itself becomes disrupted as a result [18].

X-ray and neutron reflectivity techniques are the most appropriate methods to study ultra-thin organic films [19]. Both techniques are very sensitive to changes in the scattering length density (SLD) profile normal to the interface. Such a profile can be defined with angstrom resolution [20]. When investigating biological objects, the neutron reflectivity technique is especially useful because the high penetration depth of neutrons in silicon makes it possible to perform the measurements at a solid–liquid interface, which in the first approximation can constitute an *in situ* measurement [21]. Another reason to use neutrons is that the neutron SLDs of alkyl chains, D_2O, titanium and titanium dioxide are very different. This difference yields enhanced contrast for the self-assembled monolayer of OPA.

Herein, we present X-ray and neutron specular reflectivity data to characterize the structure of this OPA - POPE coating on a titanium surface with a titanium dioxide layer.

Methods

Implants

For X-ray reflectivity measurements, the model implant surface was a layer of titanium (99.7% pure, PureTech, New York, NY, USA) that was sputtered onto a silicon substrate (DXL Darmstadt, Germany) with a polished surface.

In the neutron reflectivity experiments, the titanium was deposited on a silicon crystal (8 × 5 × 1 cm) with a polished surface provided by Siltronix Archamps Technopole (Archamps, France).

All depositions were performed at the Helmholtz Zentrum Geesthacht (HZG) using a magnetron sputter deposition chamber capable of handling large substrates [22]. The chamber was operated with a base pressure P_{base} in the range of 10^{-8} mbar and a working Ar pressure $P_{working}$ of 2×10^{-3} mbar.

The two circular (7.6 cm in diameter) magnetron sputter sources were installed into the high-vacuum sputter chamber. To ensure more homogeneous film thicknesses, the substrate was rotated about its center point. The samples were loaded through a special airlock system that allows the vacuum to remain unbroken. The nitrogen cryostat that was implemented into the chamber increases the quality of the vacuum. The temperature of the substrate during the coating process was measured using a thermostat connected to the bottom of the substrate, and it was maintained at 25±3°C. The distance between the substrate and the sputter sources was approximately 25 cm, and the angle to the substrate normal was 22.5°. The deposition speed was 0.04 nm per second, so the amount of deposited titanium can be accurately predicted according to the deposition time. However, the precise thickness of the deposited titanium layer and the thickness of the titanium dioxide layer, which forms immediately when the titanium surface is in contact with air, must be determined by X-ray (neutron) reflectometry.

Opa coating

The OPA coating procedure relies on the T-BAG (Tethering by Aggregation and Growth) technique, which is a simple method for the synthesis of self-ordered, self-assembled and continuous monolayers. The procedure was adapted from that in a previous study [23]. The samples were first cleaned with double-distilled water, then with acetone (Sigma-Aldrich Chemie GmbH, Munich, Germany) and finally with methanol (Sigma-Aldrich Chemie GmbH, Munich, Germany). The strongly bound monolayer film of OPA on the native oxide surface of the Ti samples was obtained by immersion in and the slow evaporation of dissolved OPA (Sigma-Aldrich Chemie GmbH, Munich, Germany) in dry tetrahydrofuran solution (Sigma-Aldrich Chemie GmbH, Munich, Germany). The concentration of the diluted solution was 33.4 mg of OPA in 100 mL of tetrahydrofuran. After heating the solution to 120°C for 64 hours, unbound OPA was removed by the sonication of the specimen in tetrahydrofuran and in methanol (Sigma-Aldrich Chemie GmbH, Munich, Germany). At the end of the procedure, a homogeneous OPA monolayer was formed on the metal surface.

Langmuir-blodgett deposition

The asymmetric lipid bilayer was prepared using the Langmuir-Blodgett (LB) technique. Here, we used a Nima 611 Langmuir-Blodgett Trough [24] that had a special reservoir for large-sized samples (5 × 8 × 1 cm). The monolayer of POPE lipids was formed in a LB reservoir that was filled with water between two special barriers that controlled the surface tension of the monolayer.

The formation of a lipid monolayer is based on the ability of phospholipids to orient themselves at an air/water interface to minimize their free energy and form an insoluble monolayer called a Langmuir film [25]. By dripping a dilute solution of POPE with the concentration – 1 mmol POPE per 1 L solvent (20% methanol and 80% chloroform), molecules of POPE are spread over the interface. A monolayer is established after the solvent evaporates. It is assumed that the solvent evaporation is finished when the surface tension between the barriers in the LB reservoir stabilizes. In the next step, the surface tension of the POPE monolayer is driven to 35 Nm/m^2 by changing the area between the barriers because this value corresponds to the surface tension of a lipid membrane in vivo [26].

When the POPE monolayer is in equilibrium, the deposition process begins and phospholipids are transferred to the OPA-coated Ti crystal in three steps (Figure 1).

The speeds when dipping into and out of the solution were the same and equaled 0.2 mm per second, which was the lowest speed for this device, for the first two iterations. For the third iteration, the speed was 5 mm per second, which was the highest speed for this device.

The samples containing a free-floating lipid bilayer were probed only in the neutron reflectivity experiment because they had to remain in liquid at all times after the last step of the deposition procedure.

X-ray experiment dry measurements in air

X-ray experiments were performed to check the quality of the OPA coating procedure. These experiments were performed at HZG by applying the X-ray diffractometer XRD 3003 PTS (Seifert & Co, Germany) using a Cu tube (CuKα radiation, λ=1.541 Å) and a Göbel mirror for vertical collimation onto the sample to increase intensity. The scattering plane lies here in the horizontal direction. The measured intensity of the scattered beam was corrected for small angles due to over-illumination effects by the so-called footprint correction (a detailed

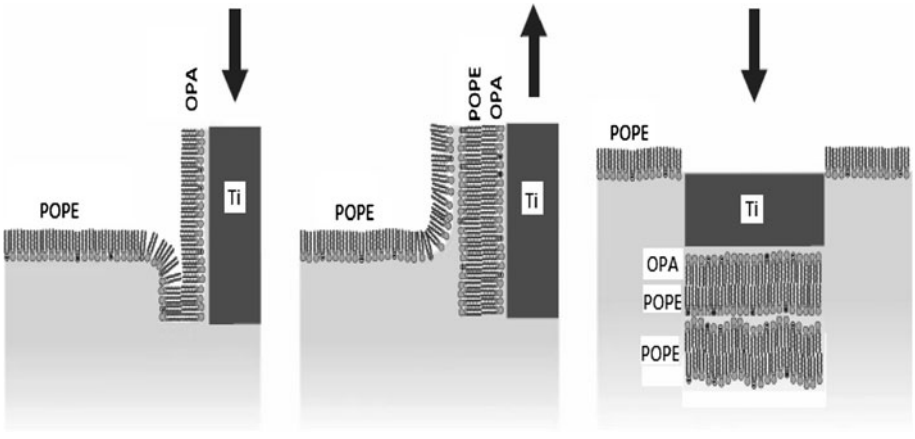

Figure 1 POPE deposition in three steps. Three steps of the deposition: The first step is the Langmuir-Blodgett transfer–the OPA coated Ti crystal, which is perpendicular to the water surface, is dipped through the monolayer of POPE lipids; The second step is the Langmuir-Blodgett transfer – the sample is moved up perpendicularly though the monolayer of POPE lipids; The third step is Langmuir-Schaefer transfer–the sample, which is parallel to the water surface, is pushed through the monolayer of lipids,. Adapted from [27].

description of the footprint correction can be found in a previous study [28]).

To extract the specular X-ray spectra, the diffuse background has to be subtracted from the measured reflectivity scan. Such a background can be recorded by performing an offset scan – a longitudinal scan with a slight offset in the θ-2θ condition ($\theta_i \neq \theta_f$) [29]. The offset in used in the experiment was equal to 0.15 degree, which was determined by rocking scans at several selected positions to ensure that we are far enough to avoid any specular contributions as well as close enough to detect the real background signal.

Neutron experiment measurement in water

Experiments were performed on the time-of-flight reflectometer Figaro (ILL, France). Two incident angles (0.624 and 3.78 degrees) were used to enable measurements of the reflectivity up to 0.3 $Å^{-1}$ in Q_z using wavelengths of the incoming beam in the range from 2 Å to 30 Å. The lambda resolution for this measurement was kept constant at 4.2% by the chopper system. The divergence of the incident angle was less than 2%, which yielded an overall dQ/Q resolution of 4.7%. For data collection, a 2D helium-3 detector was used with an active area of 500 × 250 mm^2 and a resolution of 2 mm × 7 mm. A more detailed description of the Figaro reflectometer can be found elsewhere [30].

The data treatment was performed according to a standard procedure [31].

Describing the reflectivity profile

For the data analysis, a semi-kinematic approximation is used. The reflectivity of a rough interface can be expressed as follows [32]:

$$R(Q_z) = R_F(Q_z)\left|\frac{1}{\rho_s}\int_{-\infty}^{\infty}\frac{d\rho(z)}{dz}\exp[iQ_z z]dz\right|^2$$

where ρ(z) is the scattering length density (SLD) profile along the normal direction (Z) of the surface and ρ_s is the total difference in the SLD between the two adjoining media (silicon and water or silicon and air in this experiment).

In this paper, the Motofit program [33], based on the Parratt recursion formula [34], is applied to model the extracted reflectivity curves by considering the least-squares fitting of multiple-contrast X-ray and neutron reflectivity data. For a non-Gaussian roughness as is the case for very rough interfaces, the scattering length density profile was approximated by slicing the interface into thin slabs of varying scattering length densities [20].

Scanning electron microscopy

The heat treatment of the OPA coating might have impaired the integrity of the coating. To visualize the surface, a Ti crystal to which the heat treatment was applied and a Ti+OPA coated crystal were probed by scanning electron microscope (SEM) measurements. This experiment was performed using an Auriga SEM (Zeiss, Oberkochen, Germany). SEM images were taken at a 6 kV acceleration voltage with the secondary electron (SE) detector, which produces high-resolution images of the surface. The distance between the electron gun and the surface was kept constant at 9.9 mm during the measurement. All measurements were performed under high vacuum at a pressure of 1.2 - 2.7 10^{-5} mbar.

Results and discussions

X-ray experiment

In the analysis of the uncoated substrate, the following layers must be considered to model the scattering length density profile (Table 1):

1) Silicon wafer;
2) Titanium layer; and
3) Layer of titanium dioxide.

The reference X-ray reflectivity curve for the first sample coated with pure titanium is shown in Figure 2. The fit of the curve did not require an assumption of a layer of silicon dioxide. The best fitting result is achieved with a titanium layer thickness of 636 Å and a roughness of 10 Å. The experimental curve shows a position in Q_z at which the oscillations of the metal layer disappear and that divides the oscillations into two parts. This point, which is known in the literature as a "beating point" [28], is mainly determined by the titanium dioxide layer (Figure 2). The position of the "beating point" corresponds to the thickness of the titanium dioxide. Refining the parameters to find the best fit, the thickness and roughness of the titanium dioxide layer were determined to be 36.9 Å and approximately 10 Å, respectively.

Table 1 X-Rays SLD profiles

Sample	Material	Thickness, Å	SLD, $10^{-6}Å^{-2}$	Roughness, Å
Titanium plate	air	None	0	None
	TiO_2	36.9±0.5	30±1.5	10±2
	Ti	636±2	36±1	10±2
	Si	None	20.1	3±1
Titanium plate coated with OPA	air	None	0	None
	OPA layer	23±1	8.25	10±2
	TiO_2	36.9±0.5	30±1.5	10±2
	Ti	636±2	36±1	10±2
	Si	None	20.1	3±1

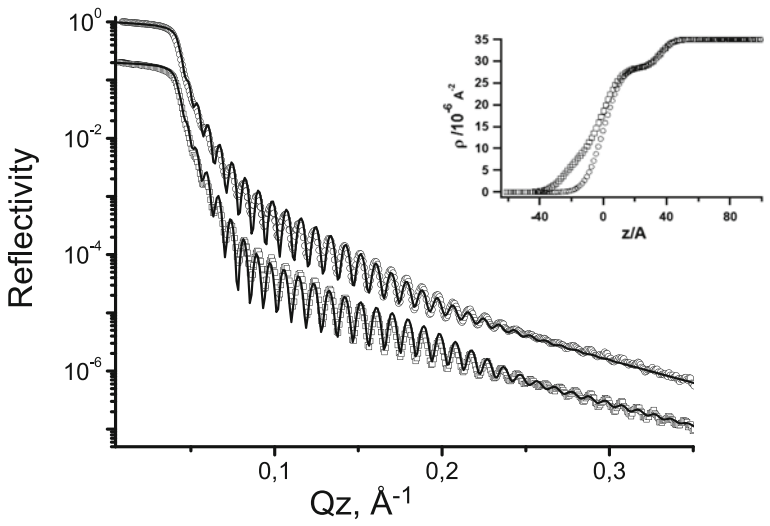

Figure 2 X-ray reflectivity experiment. The round dots correspond to the uncoated titanium plate and the cubic dots to the OPA coated titanium plate. The beating point can be observed for both experimental curve at Q_z = 0.27 Å^{-1}. The corresponding scattering length density profiles of the fits are present in the upper right corner. The reflectivity curves are offset vertically for clarity. SLD profiles of the oxide and POPE region are shown with the TiO_2/air or TiO_2/OPA interface defined as zero to enlarge the difference between the models.

A comparison of the reflectivity curves from the uncoated and OPA-coated specimens shows clearly that the curve shape has been modified (Figure 2). In the Q_z-range from 0.1 Å^{-1} to 0.2 Å^{-1}, the reflectivity of the covered plate is lower than that of the native specimen. The identical position of the "beating point" for both curves indicates that the chemical procedure did not alter the titanium dioxide layer. The reflectivity curve was fitted by adding an additional layer of OPA to the model applied to the unmodified plate (Table 1). The SLD value for the OPA layer depends on both the chemical composition of the OPA molecule and the density of the layer. The density for this layer corresponds to the density of alkyl chains of lipids in a biomembrane in the condensed phase, which has a value of 0.86 g/cm^3 and results in SLD measurements of 8.3 10^{-6}Å^{-2} and –3.1 10^{-7}Å^{-2} for X-rays and neutrons, respectively. The thickness of the OPA layer was determined to be 23 Å with a roughness of approximately 10 Å, which is in good agreement with the investigations of other authors (19–22 Å) [35,36]. Our results indicate strongly that the titanium surface was completely coated by a monolayer of OPA with the preferred dense packing.

Neutron experiment

The goal of the study is to clarify whether a biomimetic phospholipid coating comprised of several bilayers can be formed on a metal surface and whether it is stable enough to persist under physiological conditions. Neutron reflectivity experiments are ideally suited to investigate the mimetic coatings directly at a liquid–solid interface that in the first approximation matches the realistic conditions in a human body. Neutrons can probe liquid–solid interfaces due to their large penetration depth in matter. Another advantage of using neutrons as a probe is their high sensitivity to low-mass materials, which creates sufficiently large scattering contrasts to distinguish biological objects. The SLD contrast between alkyl chains, head groups and D_2O is much stronger for neutrons compared to X-rays, and this contrast enables one to study the structure in more detail.

In total, three Ti-coated samples were prepared and measured against D_2O by neutron scattering. According to the neutron data analysis, all three samples were built up in a similar fashion: a SiO_2 layer of 40 Å, a Ti layer of 368 Å and a TiO_2 layer of 24 Å having roughnesses of 8 Å, 12 Å and 13 Å, respectively. Two of the samples were coated by OPA, while the third sample was left uncoated but was otherwise treated with the same steps as the OPA samples (e.g., heating and sonication in organic solvents) as a reference to check how the mechanical stress during the OPA coating procedure affects the titanium surface.

The reference measurement of the uncoated but thermally treated Ti crystal was also performed against D_2O (Figure 3B). Comparing the reflectivity curves measured before and after the heating process, the oscillations from the titanium are shifted and have a larger periodicity, which indicates that the original titanium layer has become thinner due to the oxidation process that occurred during the heat treatment. In addition, the amplitude of the oscillations for the heat-treated specimen is

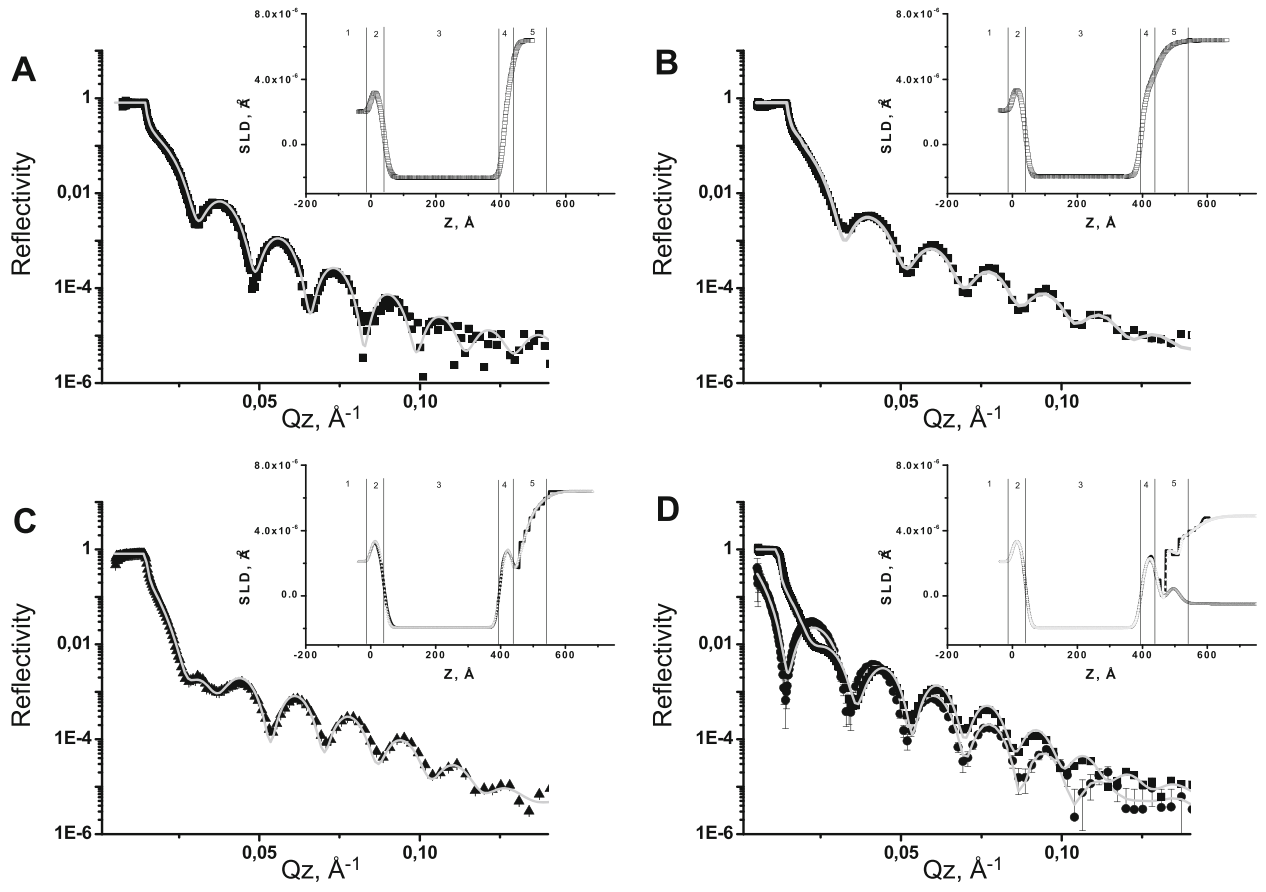

Figure 3 Neutron reflectivity experiment. A) Squares correspond to Ti crystal, which was not heated before. This curve was measured against D_2O; **B)** Squares – Ti crystal after the thermal treatment, measured against D_2O; **C)** Squares - OPA coated Ti crystal vs D_2O; **D)** Squares – Ti+OPA+POPE+2xPOPE crystal vs D_2O-H_2O mixture (80%-20%). Circles - Ti+OPA+POPE+2xPOPE crystal vs H_2O. The fits are presented in the graphs as the light grey lines. For clarity the theoretical curve obtained from the step SLD profiles are skipped, since they are quite identical to the presented theoretical curves obtained from the smooth SLD profiles. The step SLD profiles are presented **(**graphs **C** and **D)** as well as the smooth SLD profiles in the upper-right corners of the graphs. The region 1 corresponds to silicon; the region 2 – the layer of silicon dioxide; the region 3 – the layer of titanium; the region 4 – the layer of titanium dioxide. The parts of the SLD profiles, which are placed in region 5, fit the hydrocarbon region, in turn, the bumps in the region 5 correspond to the head's groups region of POPE.

smaller than the amplitude of the untreated sample. Because these two measurements were performed with the same resolution conditions, the weaker oscillation indicates an increased interfacial roughness. An analysis of the curve showed that the layer of titanium was approximately 10 Å thinner and that the top layer of titanium dioxide was 20 Å thicker than for the original specimen before heating. To obtain a proper fit of the reflectivity curve, an additional gradient in the SLD profile between the TiO_2 layer and the D_2O is required (Figure 3B). Such a gradient can originate from undesired cracks at the surface that are filled with D_2O and thus change the average SLD of the titanium dioxide layer. The average depth of such cracks can be estimated from the scattering length density profile to be approximately 40 Å, which corresponds roughly to the thickness of the titanium dioxide layer. These cracks in the TiO_2 layer could be the result of heating the sample to 120 degrees as part of the OPA coating process [23].

The unmodified but heat-treated Ti crystal was probed using SEM. In contrast to the SEM images of a freshly prepared crystal before heating, these images revealed that some cracks were present on the surface (Figure 4) with typical widths in the range of 300 nm. The occurrence of cracks may result from the thermal expansion coefficient for titanium (titanium dioxide), which is three times larger than that for silicon ($9\ 10^{-6}$ and $3\ 10^{-6}$°C^{-1}, respectively [37]). This effect was not observed in the X-ray reflectivity experiments because the silicon wafers used for the titanium deposition were ten times thinner than the silicon crystals used as specimens in the neutron experiment. At one-tenth of the thickness, the

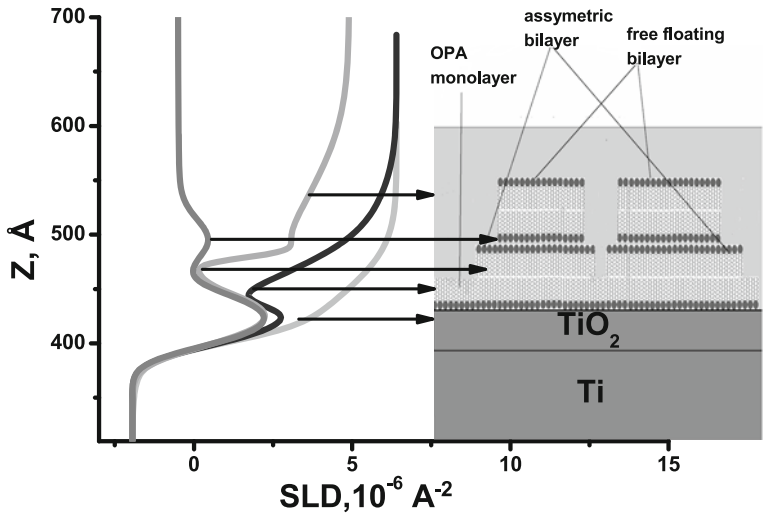

Figure 4 Typical SEM pictures of the Ti crystal before heating (left), after heating (right).

tensile force applied to the titanium coating during the heating process was also ten times weaker and was obviously not strong enough to cause cracks to develop.

The two OPA-coated crystals were also probed against D_2O to vary the contrast in the system. Both crystals produced similar reflectivity curves. That demonstrates the excellent reproducibility of the sample preparation. By comparing the reflectivity curves of the unmodified Ti crystal to the OPA-coated specimens, as shown in Figure 3C, the following changes in the curve shape are observed in the region below 0.07 $Å^{-1}$:

1) The intensity of the reflectivity curve of the coated crystal decays faster than for the uncoated one.
2) The first oscillation of the OPA-coated crystal is split into two oscillations at Q_z=0.032 $Å^{-1}$ and Q_z=0.044 $Å^{-1}$ (Figure 3C).

For Q_z higher than 0.07 $Å^{-1}$, the reflectivity curves have almost the same shape to within the background noise.

Due to the relatively high roughness of the initial surface the roughness of the OPA monolayer is also high and comparable to the thickness of the OPA monolayer. In this case the slicing modeling has to be applied to build a step SLD profile as it is shown in Figure 3C. The reduction of the step size leads to a smooth SLD profile. Careful modeling of the curve for the OPA-coated titanium crystal showed that this smooth SLD profile can be obtained by adding only one rough layer to the SLD profile of the heated Ti crystal to represent the OPA monolayer. The SLD of this additional layer corresponds to the SLD of CH_2 groups at the density of the alkyl chains of the lipid membrane in the condensed phase (0.86 g/cm^3). The thickness of the OPA layer was found to be 24 Å.

For the analysis of the reference curve, a gradient has to be chosen to make a satisfactory model fit (Table 2). To check the surface for cracks, the Ti+OPA crystal was also probed by SEM. Indeed, the SEM images show similar cracks on the surface as the heated Ti crystal. The thickness and packing density perfectly match the results obtained from the X-ray data described earlier, and these two independent experiments both indicate the presence of a well-ordered and uniform SAM of OPA on the titanium surface.

As the next step, a system was prepared consisting of an asymmetric bilayer of OPA plus POPE with an additional free-floating POPE bilayer. During the measurements, the sample's temperature was maintained at 20°C by the attached thermostat. At this temperature, the POPE lipids remained in the gel phase, which leads to a better ordered monolayer structure than in the case of the liquid crystalline state.

The sample was inserted into its cell directly after the Langmuir-Schaefer transfer in the LB bath with H_2O. Then, the H_2O in the sample cell was exchanged with D_2O. To perform this exchange, we injected a volume of D_2O into the chamber 5 times greater than the volume of the cell. However, the critical angle, which becomes shifted, indicates that some H_2O continues to be present in the sample chamber due to incomplete H_2O-D_2O exchange. The reflectivity curve of the Ti+OPA+POPE+2xPOPE crystal could be successfully fitted by assuming that a D_2O-H_2O mixture (80%-20%) was present in this measurement (Table 2 and the SLD profile in Figure 3 and Figure 5).

Another important feature is the slight shift of the oscillations to the region of smaller Q_z when compared to the OPA-coated sample (Figure 3D). This shift indicates the presence of an additional coating layer on top of the OPA layer.

Table 2 Neutron scattering length densities

Sample	Material	Thickness, Å	SLD,10^{-6}Å^{-2}	Roughness, Å	Solvent volume fraction, %
Ti crystal before heating vs D_2O	Si	None	2	None	0
	SiO_2	40±2	3.4	8±4	0
	Ti	368±3	−1.96	12±2	0
	TiO_2	24±2	2.4	13±2	0
	Subphase layer	None	6.36	15±5	
	D_2O	None	6.36	0	
Ti crystal after heating vs D_2O	Si	None	2	None	0
	SiO_2	40±5	3.4	8±4	0
	Ti	357±2	−1.96	12±2	0
	TiO_2	38±3	2.4	13±2	12±5
	D_2O	None	6.36	13	
OPA coated Ti crystal vs D_2O	Si	None	2	None	0
	SiO_2	40±5	3.4	8±4	0
	Ti	357±2	−1.96	12±2	0
	TiO_2	40±5	2.9	13±2	12±5
	OPA layer	24±1	−0.3	12±2	12±5
	Gradient layer	60±10	6.36	60±10	
	D_2O	None	6.36	0	
Ti+OPA+POPE+2x POPE bilayer vs D_2O- H_2O mixture (80–20)	Si	None	2	None	0
	SiO_2	40±5	3.4	8±4	0
	Ti	357±2	−1.96	12±2	0
	TiO_2	40±5	2.9	13±2	12±5
	OPA	24±1	−0.3	12±2	12±5
	Chain's group region 1	17±2	1.5±0.4	12±4	32±5
	Head's group region 1	16±2	2.6±0.4	5±2	32±5
	Chain's group region 2	34±3	2.2±0.4	10±3	53±5
	Head's group region 2	8±1	3.4±0.4	5±3	53±5
	Gradient layer	60	4.9	60	
	D_2O	None	4.9	0	
Ti+OPA+POPE+2x POPE vs H_2O	Si	None	2	None	0
	SiO_2	40±5	3.4	8±4	0
	Ti	357±2	−1.96	12±2	0
	TiO_2	40±5	2.9	13±2	12±5
	OPA	24±1	−0.3	12±2	12±5
	Chain's group region 1	17±2	−0.3±0.4	12±4	32±5
	Head's group region 1	16±2	1.2±0.4	5±2	32±5
	Chain's group region 2	34±3	−0.4±0.1	10±3	53±5
	Head's group region 2	8±1	0.5±0.3	5±3	53±5
	Gradient layer	60	−0.5	60	
	D_2O	None	−0.5	0	

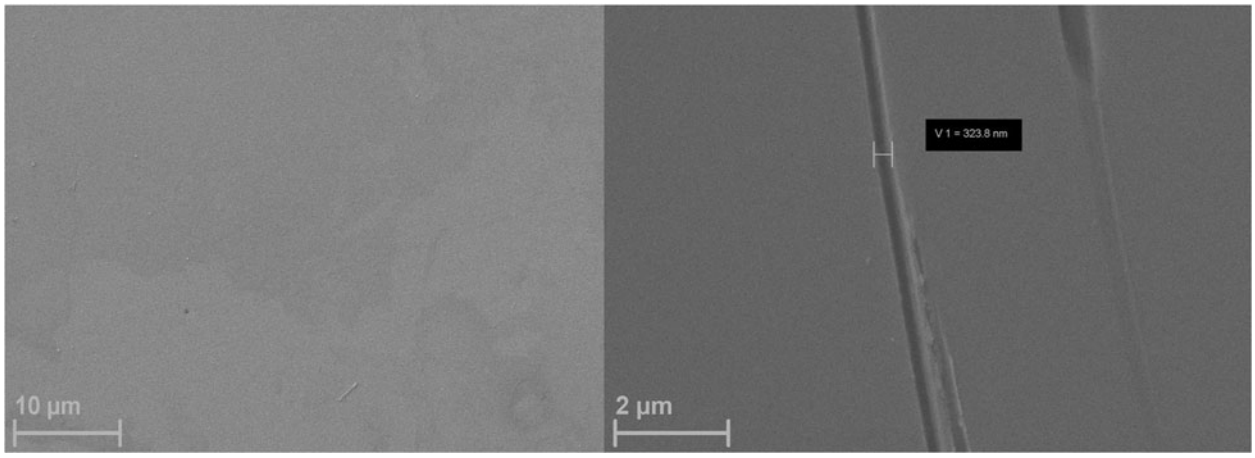

Figure 5 Zoomed neutron SLD profiles and their correlations to the real surface.

Supporting the assumption of an additional phospholipid coating on the OPA-coated crystal, the first two oscillations at Q_z=0.032 $Å^{-1}$ and Q_z=0.044 $Å^{-1}$ become more pronounced in comparison to the corresponding oscillations of the reflectivity curve of the Ti+OPA crystal. According to the simulation, such a change in the shape of the reflectivity curve corresponds to an increased thickness of the hydrogen-rich region between the titanium dioxide and the contrast mixture at the solid–liquid interface by 30 Å to 40 Å.

As in the case of the OPA-coated titanium crystal the slicing procedure has also to be applied for the analysis of the Ti+OPA+POPE+2xPOPE reflectivity curve resulting in a step like SLD profile (see Figure 3D). By increasing the number of slices the calculated SLD profile converges more and more with a smooth SLD profile (see Figure 3D), By taking into account the known size and SLD values of the molecules presented on the surface, the smooth SLD profiles indicate that the roughnesses of the layers are in order of their thicknesses. Even though the transition between the different materials in the SLD profile can not be described by a perfect Gaussian distribution in these cases, it is still possible here to approximate the rms roughness values (σ) for such interfaces by reasonable fits using the Gaussian distribution leading to the values listed in Table 2. The model of the Ti+OPA+POPE+2xPOPE crystal considers all three steps of the POPE deposition (Figure 1 and Table 2). The fitting parameters for the first five layers (up to the OPA layer) are fixed at the values obtained from the fit of the OPA-coated crystal. The water layer between the POPE monolayer adjacent to the OPA and the next POPE bilayer cannot be distinguished within the data because this water layer is only a few angstroms thick and the border area the SLD profile is smeared out due to the cracks in the TiO_2 layer. These two head group regions and the water layer are combined into one box-layer titled "Head group region 1". The layer "Head group region 2" also combines the PE region and the absorbed D_2O molecules. The analysis is carried out in the rough approximation that the amount of the absorbed D_2O molecules is the same for each head group regions, so the thickness of the "Head group region 1" is precisely twice the thickness of the "Head group region2". The analysis of this curve focused on the determination of SLD values and roughnesses to provide information about the quality of the coating at each step of the deposition. The thicknesses of the tail group and the head group were kept fixed at 34 Å and 8 Å, respectively, in agreement with values from the literature [38,39] where a DPPE lipid was deposited in a similar way onto silicon and quartz surfaces. Our fits show, however, that the measured SLD for the tail region may be higher due to an incomplete coating that contains heavy water molecules. From the values of SLD, it is possible to predict the percent coating of the surface using the following calculation:

$$\rho_{\text{measured}} = \phi\rho_{\text{tails}} + (1-\phi)\rho_{\text{contrast}}$$

where ϕ is a volume fraction of the solvent with the corresponded SLD ρ_{contrast} in the hydrocarbon region (ρ_{tails}).

Using this equation leads to a LB deposition of approximately 65% and a Langmuir-Schaefer transfer of 45%. This model is confirmed by the analysis of the second reflectivity curve for the Ti+OPA+POPE+2xPOPE crystal, which was performed in H_2O. Such an incomplete coating has been observed, for example, by Rondelli [40], who has shown that similarly deposited DSPC-cholesterol bilayers on a silicon block contain 40% water.

Conclusions

In this paper, a structural analysis of a new implant material is presented. N-octadecylphosphoric acid was chemically deposited onto titanium surfaces and probed by X-ray and neutron specular reflectivity experiments. It was demonstrated that a well-ordered monolayer of OPA forms on the surfaces as a result of the OPA deposition procedure. The values for the thickness (24 Å) and the roughness (8 Å) of the self-assembled OPA layer were confirmed independently by X-ray and neutron specular reflectivity techniques.

The OPA+POPE+2xPOPE coating was examined at the solid/liquid interface in a neutron reflectivity experiment. The analysis of the neutron data clearly reveals that Langmuir-Blodgett deposition of POPE lipids on top of the modified titanium surface leads to a POPE monolayer that coats 65% of the surface. Our fits also show that an additional free-floating lipid bilayer coats approximately 45% of the surface.

The presence of a POPE coating surrounding a real implant material is an important result with respect to the biomimetic requirements of implant surfaces. Previously, most reflectivity investigations were focused on a solid-supported bilayer on top of the silicon and quartz surfaces. Moreover, POPE lipid is not usually used for such an investigation because unsaturated hydrocarbon chains lead to an unstable bilayer, which is not easy to handle. To the best of our knowledge, this is the first time that a biologically relevant surface on a model implant has been described by X-ray and neutron reflectometry techniques. All of our findings demonstrate that the OPA+POPE+2xPOPE coating is a very promising combination for the development of future titanium implants.

Abbreviations

POPE: Phospholipid 1-palmitoyl-2-oleoyl-sn-glycero-3-phospho-ethanolamine; OPA: n-Octadecylphosphonic acid; SLD: Scattering length density; SEM: Scanning electron microscope; LB: Langmuir-Blodgett.

Competing interests

The authors declare that they have no competing interests.

Authors' contributions

MG carried out the data collection, performed the data analysis and wrote the manuscript. DL helped to draft the manuscript. EW was the instrument responsible person. VG, BL and AS took a part in the discussion of the data. MS performed the preparation of the model implant surfaces. RG gave the final approval of the version to be published. All authors read and approved the final manuscript.

Acknowledgments

The authors would like to thank technicians from the chemical lab of HZG Daniela Lange and Gabriele Salamon for their help in the preparation of the samples.
The article is an original publication.

Author details

[1]Institute of Materials Research, Helmholtz-Zentrum Geesthacht Zentrum für Material und Küstenforschung (HZG), Geesthacht, Germany. [2]Institute Laue-Langevin (ILL), Grenoble, France.

Received: 12 June 2013 Accepted: 12 August 2013
Published: 19 August 2013

References

1. Bosco R, et al. (2012) Surface Engineering for Bon Implants: A Trend from Passive to Active Surfaces. Coatings 2:95–119
2. Zethraeus N, et al. (2007) Cost-effectiveness of the treatment and prevention of osteoporosis. Oseoposros Int 18:2–23
3. Roach HI, et al. (2007) Pathobiology of asteoarthritis: pathomechanisms and potential therapeutic targets. Current Drug Targets 8(2):271–282
4. Barrere F, et al. (2008) Advanced biomaterials for skeletal tissues regeneration: Instructive and smart functions. Mater Sci Eng Rep 59:38–71
5. Borovecki F, et al. (2007) Biological mechanisms of bone and cartilage remodelling–genomic perspective. Int Orthop 31(6):799–805
6. Williams DF (2008) On the mechanism of biocompatibility. Biomaterials 29:2941–2953
7. Tengvall P (1992) Physico-chemical consideration of titanium as biomaterial. Clin Mater 9:115–134
8. Singhatanadgit W (2009) Biological Responses to New Advanced Surgace Modifications of Endosseous Medical Implants. Bone and Tissue Regeneration Insights 2:1–11
9. Santin M, et al. (2006) Calcium-Binding Phospolipids as a Coating Material for Implant Osteointergration J R Soc. Interface 3(7):277–281
10. Bosetti M, et al. (2007) Cell Behaviour on Phospolipids-Coated Surfaces. Mater Sci Mater Med 18(4):611–617
11. Willumeit R, et al. (2007) Phospholipids as Implant Coatings. Mater Sci Mater Med 18:367–380
12. Willumeit R, et al. (2007) In-Vitro Interactions of Human Chondrocytes and Mesenchymal Stem Cells, and of Mouse Macrophages with Phospholipid-Covered Matallic Implant Materials. Eur Cell Mater J 13:11–25
13. Kochanowski A, et al. (2010) Examination of the Inflammatory Response Following Implatation of Titanium Plates Coated with Phospholipids in Rats. J Mater Sci: Mater Med 22(4):1015–1026
14. Gao W, et al. (1996) Self-Assembled Monolayers of Alkylphosphonic Acids on Metal Oxides. Langmuir 12(26):6429–6435
15. Fabre RM, et al. (2009) Stable Supported Lipid Bilayers on Zirconium Phosphonate Surfaces. Langmuir 25(21):12644–12652
16. Willumeit R, et al. (2004) Biological Multi-layer Systems as Implant Surface Modification. Materialwissensschaft und Werkstofftechnik 34(12):1084–1093
17. Vance JE (2012) Formation and Function of Phosphatidylserine and Phosphadylethanolamine in Mannalian Cells. Biochimica et Biophysica Acta 1831(3):543–554
18. Wellner N, et al. (2012) N-acylation of phosphatidetethanolamine and its biological function in mammals. Biochim Biophys Acta 12:1388–1981
19. Russell TP (1996) On the Reflectivity of Polymers: Neutrons and X-rays. Physica B 221(1-4):267–283
20. Zaber H (1994) X-ray and Neutron Reflectivity Analysis of Thin Flms and Superlattices. Appl Phys A 58:159–168
21. Petrash S, et al. (1997) Neurtron and X-ray REflectivity Studies of Human Serum Albumin Adsorption onto Functionalized Surfaces of Self-Assembled Monolayers. Biotechnol Prog 13:635–639
22. Stoermer M, et al. (2007) Structure and Corrosion of Magnetron Sputtered PUre Mg Film on Silicn Substrates. Plasma Processes and Polymers 4(1):557–561
23. Gawalt ES, et al. (2001) Self-Assembly and Bonding of Alkanephosphonic Acids on the Native OXide Surface of Titanium. Langmuir 12:5736–5738
24. Nima K (2013) Lanmuir and Langmuir-Blodgett Troughs. http://www.ksvnima.com/products/langmuir-and-langmuir-blodgett-troughs
25. Agnes PG-E, et al. (2007) Langmuir-Blodgett Technique for Synthesis of Biomimetic Lipid Membranes. Fundamental Biomedical Technologies 1:23–74
26. Quinn PJ, Wolf C (2009) The liquid-ordered phase in membranes. Biochim Biophys Acta 1788(1):33–46
27. Fragneto G, et al. (2012) Floating Lipid Bilayers: Models for Physics and Biology. Eur Biophys J 41(10):863–874

28. Daillant J (1999) X-Ray and Neutron Reflectivity: Principles and Applications. Lecture Notes in Physics: N.s. M, Monographs 58:87–121
29. Salditt T, et al. (2002) Europhys. JE 7(105):7105
30. Campbell RA (2011) The New Horizontal Neutron Reflectometer at the ILL. The European Physical Journal Plus 126(11):107–108
31. Ott F, Kozhevnikov S (2011) Off-Specular Data Representations in Neutron Reflectivity. J Appl Crystallogr 44:359–369
32. Constantin D, et al. (2003) Solid-supported lipid multilayers: structure factor and fluctuations. Eur Phys J E Soft Matter 12(2):283–290
33. Nelson A (2006) Co-Refinement of Multiple-Contrast Neruton/X-ray reflctvity data using MOTOFIT. J Appl Crystallogr 39:273–276
34. Parratt LG (1954) Surface Studies of Solids by Total Reflection of X-Rays. Phys Rev Lett 95(2):359–369
35. Nie HY, et al. (2008) Optical Properties of an Octadecylphosphonic Acid Self-Assembled Monolayer on a Silicon Wafer. Thin Solid Films 517:814–818
36. Woodward JT, et al. (1996) Self-Assembled Monolayer Growth on Cctadecylphosphonic Acid on Mica. Langmuir 12:3626–3629
37. Tipler PA, Mosca G (2008) Mechanics, Oscillations and Waves, Thermodynamics. Physics for Scientists and Engineers 1, 6th edition. Worth Publishers, New York, NY, pp 666–670
38. Stidder B, et al. (2006) Structure and Stability of DPPE planar bilayers. Soft Mater 3:214–222
39. Fragneto G, et al. (2001) A Fluid Floating Bilayer. Europhys Lett 53(1):100–106
40. Rondelli V (2012) Reflectivity from Floating Bilayers: Can We Keep the Srtuctural Asymmetry. Journal of Physics: Conference Series 340

doi:10.1186/1559-4106-8-21
Cite this article as: Golub *et al.*: X-ray and neutron investigation of self-assembled lipid layers on a titanium surface . *Biointerphases* 2013 **8**:21.